Journal of Power Sources 196 (2011) 7550–7554

Contents lists available at ScienceDirect

Journal of Power Sources

journal homepage: www.elsevier.com/locate/jpowsour

Impact of land width and channel span on fuel cell performance

Steven G. Goebel*

Fuel Cell Activities, General Motors Company, 10 Carriage St., Honeoye Falls, NY 14472, USA

ARTICLE INFO

Article history:
Received 1 March 2011
Received in revised form 2 April 2011
Accepted 4 April 2011
Available online 15 April 2011

Keywords:
Fuel cell
PEM fuel cell
Flow field design
Land width
Channel span
Cell performance

ABSTRACT

The impact of land width and channel span on fuel cell performance was tested on 50 cm^2 flow fields. Combinations of land widths and channel spans of 0.25, 0.5 and 1.0 mm were evaluated. Polarization curves and high-frequency resistance were measured for several humidity levels for each of the flow fields. For performance at high current density, the land width was found to be the dominant factor. Reductions to the smallest size tested (0.25 mm) continued to showed improvement over wider lands. Adequate land fraction (preferably about 50%) needs to be provided to minimize contact resistance.

1. Introduction

Fuel cells for automotive applications must provide for the normal fuel cell functions and also meet some very challenging requirements for cost, size, limited heat rejection capability and rapid cold starting. One of the elements needed for a fuel cell is a separator plate. Based on cost and size, the most favorable approach is to use stamped metal plates. As the total stack cost is scaled by the needed power, it is important to achieve the highest power per material that is used. Aspects of the plate design that affect performance (and therefore cost) include: uniform flow to each cell and within the cells, diffusion distance across lands, distribution of humidity within the cell, removal of liquid water, conduction to the next cell (which is provided by the metal plate material including any conductive coatings), and electrode to diffusion media contact over channel spans. Heat rejection, for a given power output, also requires the highest possible cell voltage. To reduce the stack thermal mass to improve cold start time, a nested configuration [1] is particularly effective in reducing coolant thermal mass which is the most significant portion of the total stack thermal mass. This nested configuration requires a straight channel layout which is also beneficial for minimizing pressure drop and therefore parasitic compressor loads. Stamped plates limit channel depth based on metal forming stretch which increases pressure drop. To meet automotive system pressure drop requirements with stamped plates, straight channels are necessary as they provide the shortest possible channel length for the required active area size and can be seen in several examples of automotive fuel cells [2–4]. The system must allow adequate pressure drop to ensure good cell-to-cell and channel-to-channel flow distribution and pressure drop is also beneficial towards moving liquid water. The straight channel configuration is also suitable for a cathode to anode counter flow arrangement which is beneficial towards improving internal cell humidity uniformity and therefore performance. Within this stamped plate configuration, the remaining design parameters which affect performance are the land width and channel span.

As gas must diffuse under the lands to reach the electrode and liquid water must be moved to the channels, it is expected that fuel cell plates with narrow lands would perform better especially with regard to mass transport resistance. Although, for a half land width similar to the diffusion media thickness, further reductions in land width would not be expected to provide significant performance benefits as the diffusion (or water removal) distance would become primarily limited by the diffusion media thickness. As contact resistance also plays a role in cell performance, adequate land area or land fraction must be provided to achieve low contact resistance at an acceptable mechanical load. The channel spans also need to be narrow for the diffusion media to maintain contact with the electrode across the channel span. The competing aspects of these parameters require optimization with the specific materials and operating conditions of a particular application.

Several published works have investigated the impact of land widths and channel spans on fuel cell performance [5–8]. It was found that performance improved for the narrowest land width

* Tel.: +1 585 683 8208; fax: +1 585 624 6680.
E-mail address: steven.goebel@gm.com

0378-7753/$ – see front matter © 2011 Elsevier B.V. All rights reserved.
doi:10.1016/j.jpowsour.2011.04.005

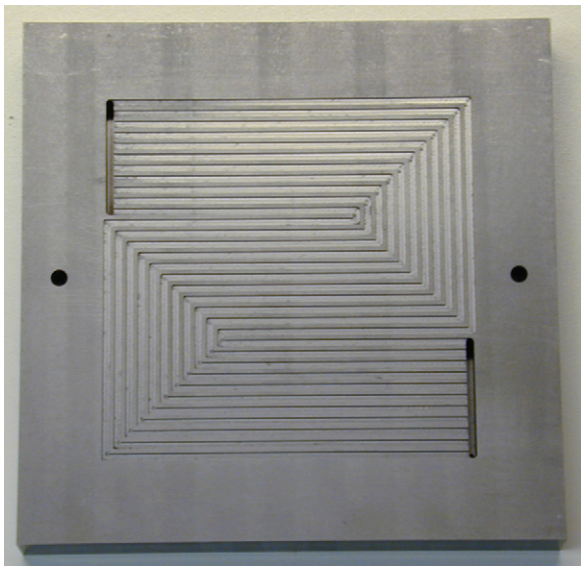

Fig. 1. Photograph of a grouped three-pass flow field.

tested of 0.5 mm [5]. Cells with higher land fractions were found to have the better performance [6], but the resistance values reported for these cells were relatively high, so contact resistance would have been important for these cell materials, design and operating conditions. Novel experiments have been done to directly and independently measure the performance in channels and under lands [7,8]. These studies found higher performance under the lands compared to the channels for wider channels at higher voltages. The narrowest channels and lands studied of 1 mm provided the highest performance.

This present study provides a number of important developments beyond what has previously been reported including: smaller land widths and channel spans to find higher performance limits, systematic combinations of land widths, channel spans, land fractions and relative humidity conditions to infer the relative importance of each flow field parameter to performance over a range of relative humidity conditions. The cell high-frequency resistance (HFR) is also reported to gain insight into performance differences between flow field configurations. This systematic data set may also be suitable for quantifying the effects of flow field parameters and for use in fuel cell flow field model validation.

2. Test method

Several 50 cm^2 flow field configurations with a selected range and combination of land widths and channel spans from 0.25 to 1.0 mm as listed in Table 1 were machined from carbon composite blocks. The channel depth for each flow field was adjusted to achieve similar pressure drop for each of the configurations. The designed channel depth needed to account for the total channel flow area. Some channel depth adjustments were also made for the smaller channels to compensate for the effect of hydraulic diameter on pressure drop. The measured pressure drops (scaled to 1.5 A cm^{-2} for comparison at the same volume flow rate) are also listed in Table 1. To better replicate the channel velocity and pressure drop of a full sized flow field, a channel length of about 21 cm was obtained by using a 3-pass arrangement as shown in Fig. 1. The channels were grouped together to minimize flow over lands between passes as this over land flow is limited in the straight channels used in full sized flow fields. In the plot legends, these flow fields are listed by land width followed by channel span.

For the diffusion media (DM), SGL25BC was used which is about 230 μm thick uncompressed, and was built to a fixed compression of 178 μm which was set by the thickness of the solid Teflon gaskets that framed its perimeter. As this diffusion media thickness was greater than half the land width of the narrowest land (half of 0.25 mm), it was expected that a performance plateau would be observed for this narrowest land width as the diffusion distance to the center of the land is becoming less than the diffusion distance through the DM thickness. For the membrane electrode assembly (MEA), 18 μm thick Gore 5510 membranes were used which had a catalyst loading of 0.4 mg-Pt cm^{-2} on both the anode and cathode sides.

For the series of tests, five samples of softgoods (DM, MEA and gasket) were used. After assembly, compression and operation, a set of these components became bonded and could be reused without disassembly in each flow field. The same sets of softgoods were used for all flow fields to ensure differences in the results were due to flow field effects and not softgood variations. For each softgood sample, the run order of the flow fields was randomized. The results for each flow field at each test condition were averaged for all sets of softgoods and repeated tests to minimize the impact of softgood variation and test repeatability on the flow field effects.

The fuel cells were operated at ambient outlet pressure with a stoichiometry of 2.0 and an inlet relative humidity of 50% for both the anode and cathode and were configured in a counter-flow orientation. A range of operating temperatures of 50, 70 and 80 °C were tested to evaluate the impact of outlet relative humidity, which were about 173, 91 and 73%, respectively, to cover a range of membrane humidification levels. A range of relative humidity was included to understand the interaction with flow field parameters, performance sensitivities and as operating conditions are limited by system capabilities such as hot and dry operation due to limited heat rejection capability and cold and wet operation during a cold start. The outlet relative humidity was based on the combined outlets of both anode and cathode. Relative humidity cannot exceed 100%, so calculated values above this indicate the amount of liquid water produced or can be used infer of the fraction of the active area that is in excess of 100% relative humidity where liquid water may inhibit gas mass transport. For the 173% outlet relative humidity conditions with 50% inlet relative humidity, (173–100)/(173–50) = 59% of the active area is above 100% relative humidity – although with counter-flow and humidity exchange between the anode and cathode, this region would be larger. Constant cell voltages of 0.65, 0.60, 0.55, 0.5 and 0.4 were tested to determine the cell's current density performance capability. Constant voltage operation was used at higher power as it was not known prior to testing what current density performance capability each flow field would have. A low power point at a fixed current density of 0.2 A cm^{-2} was also run. The test stand also provided high-frequency resistance (HFR) at 1 kHz which was useful towards interpreting some of the results.

3. Results and discussion

The polarization curves (cell voltage, *V*, vs. current density, *i*) and HFR (open symbols and dashed lines) for all of the flow fields are shown in Figs. 2–4 for 50, 70 and 80 °C conditions, respectively. A smaller symbol size was selected for the smaller land widths, and a common symbol shape was selected for each of the land fractions (even for different land widths) to facilitate interpretation of the plots. These data show the strongest effect of land width on performance. The flow fields with narrower land widths produced higher current densities for all cell voltages at all operating conditions. This difference is most pronounced at higher current densities and wetter conditions where mass transport resistance becomes important

Table 1
Details of the flow fields.

Flow field	Land width (mm)	Channel span (mm)	Channel depth (mm)	Number of channels	Land fraction	Pressure drop (kPa)[a]
0.25–0.25	0.25	0.25	0.34	48	0.50	21.5
0.25–0.5	0.25	0.50	0.25	32	0.33	25.6
0.5–0.25	0.50	0.25	0.44	32	0.67	21.6
0.5–0.5	0.50	0.50	0.28	24	0.50	29.3
0.5–1.0	0.50	1.00	0.23	16	0.33	23.4
1.0–0.5	1.00	0.50	0.44	16	0.67	13.6
1.0–1.0	1.00	1.00	0.28	12	0.50	25.3

[a] Pressure drops were scaled to 1.5 A cm^{-2} volumetric flow rates.

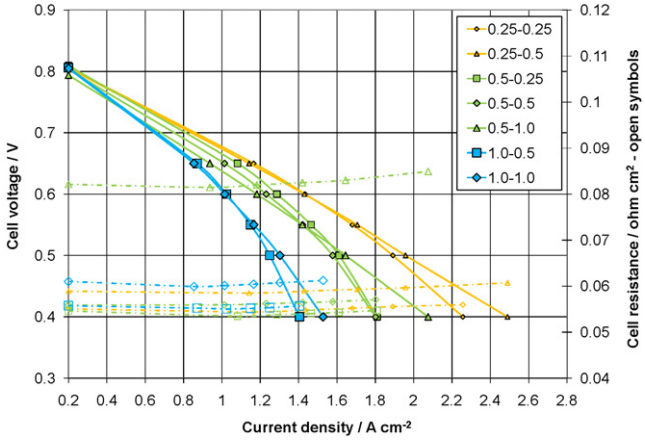

Fig. 2. Cell voltage and cell resistance at 50 °C.

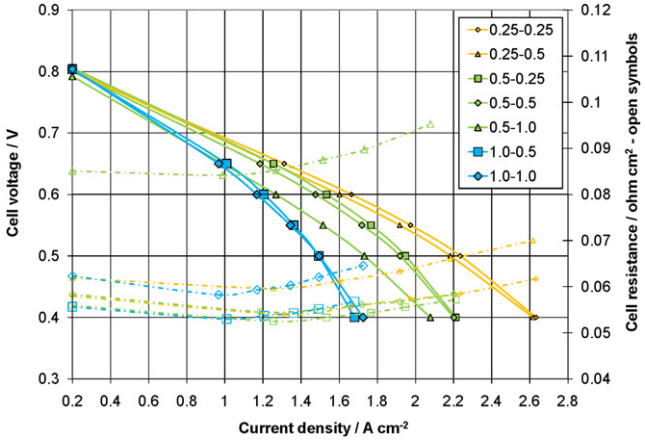

Fig. 3. Cell voltage and cell resistance at 70 °C.

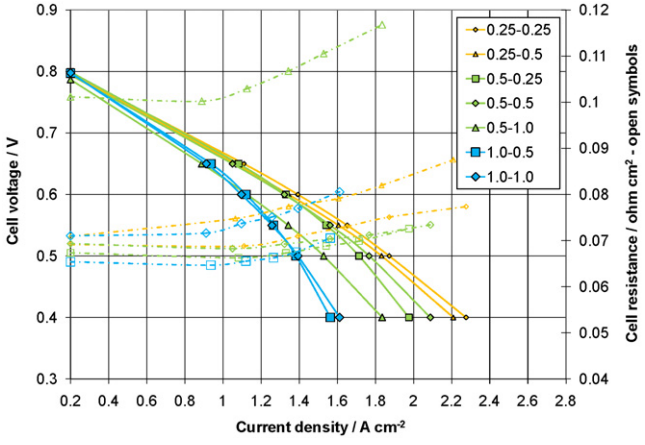

Fig. 4. Cell voltage and cell resistance at 80 °C.

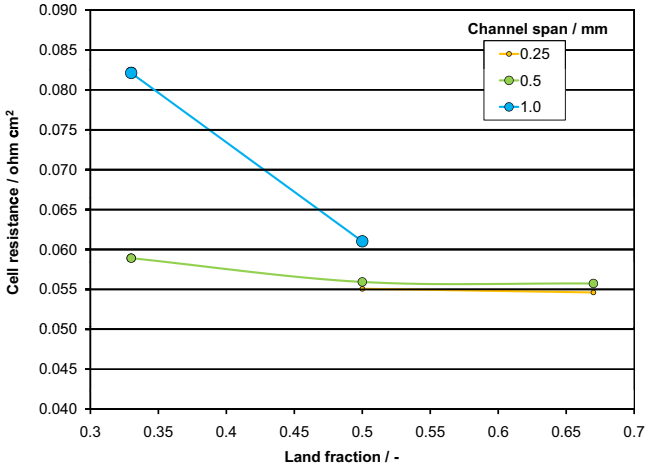

Fig. 5. Cell resistance vs. land fraction and channel span at 0.2 A cm^{-2} and 50 °C.

(where the polarization curves start to "droop") due to the diffusion resistance (distance) under wider lands and due to the water within the DM under wetter conditions.

The highest performance was achieved at 70 °C (or about 91% outlet relative humidity) conditions. The optimum operating condition is a balance between membrane hydration for proton conductivity and mass transfer resistance due to condensed water.

There is also an interaction between land fraction and operating conditions where smaller land fraction flow fields (triangle symbols) performed better at limiting currents (low voltages) under wetter conditions (50 °C), but had lower performance than the larger land fraction flow fields at drier conditions (70 and 80 °C). At higher voltages and drier conditions, larger land fraction flow fields performed better than smaller land fraction flow fields for equivalent land widths as contact resistance becomes more important than mass transport resistance although these differences were small.

Due to contact area and compression, flow fields with lower land fractions and wider channel spans had higher HFR (which reduced performance). The 0.5–1.0 land–channel flow field, which had both lower land fraction and wider channels, was considerably higher in HFR. These trends are more clearly illustrated in Fig. 5 which shows the HFR values at 0.2 A cm^{-2} for the 50 °C condition. The wettest condition was selected to better isolate the effects of electrical resistance from membrane proton resistance which is higher under drier conditions. Increases in HFR were expected due to reduced contact area between the DM and flow field for lower land fractions and due to reduced contact pressure to the MEA across wider channel spans. However, the strong interaction between channel span and land fraction was not expected. Similar behavior was observed in [6], where the flow field with the widest channel span at low land fraction had considerably higher HFR than the other flow fields. The cells for the present study were built with fixed displacement gaskets, so this may have limited the compressive load for a flow field

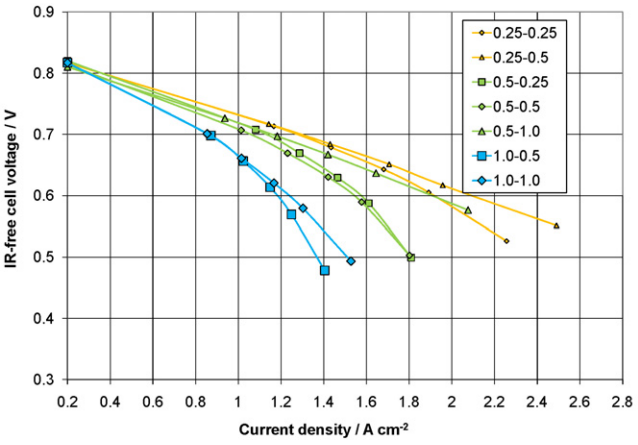

Fig. 6. IR-free cell voltage ($V + i \times$ HFR) at 50 °C.

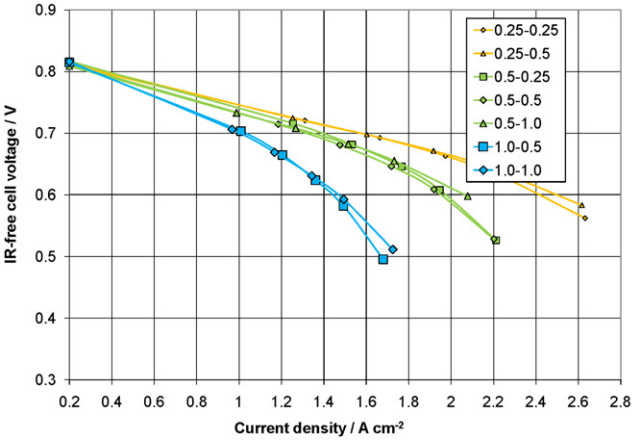

Fig. 7. IR-free cell voltage ($V + i \times$ HFR) at 70 °C.

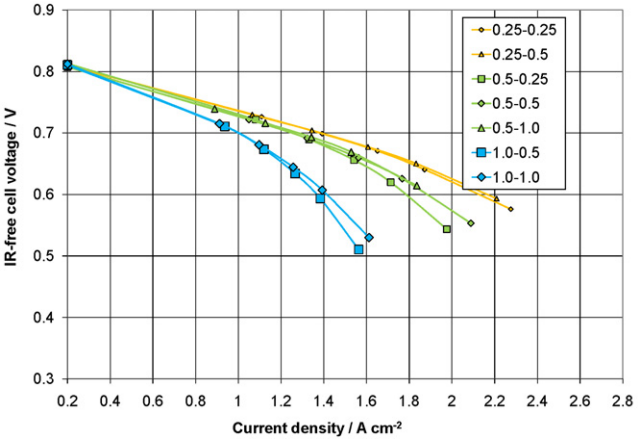

Fig. 8. IR-free cell voltage ($V + i \times$ HFR) at 80 °C.

with a low land fraction. Higher compression loads could be used to compensate for a flow field with a low land fraction, but it is undesirable for the local compressive strain to exceed the DM material strength and cause local DM fiber damage.

To better isolate the impact of mass transport resistance due to land width, the HFR loss ($V + i \times$ HFR) was removed as shown by the IR-free cell voltages in Figs. 6–8 for 50, 70 and 80 °C conditions, respectively. The relative mass transport performance of lands and channels can be inferred from the performance differences between different land fractions for each land width. Under wetter conditions, the lower land fraction flow fields performed much better indicating increased mass transport resistance under the lands for wetter conditions. The performance differences due to land fraction were much smaller under drier conditions as demonstrated in Figs. 7 and 8.

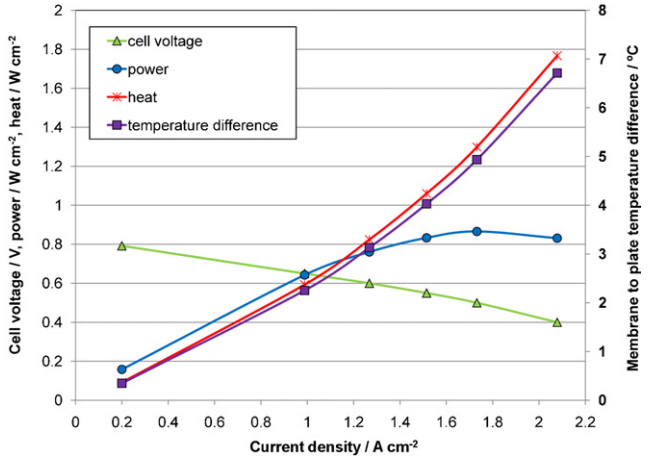

Fig. 9. Cell voltage, power, heat generation and membrane to flow field temperature difference estimate at 70 °C for the 0.5–1.0 land–channel flow field.

There were also some interesting and unexpected trends in HFR vs. current density especially for the drier conditions where the HFR values initially dropped and then increased considerably at higher current densities (lower voltages). The initial drop may be due to the increased rate of water production with current density which humidifies the membrane under these dry conditions. However, at even higher current densities and lower cell voltages, the heat generation increases at a rate faster than the water production. At higher heat generation rates, the membrane becomes much hotter than the flow field temperature (over 6 °C for the conditions shown in Fig. 9). The net effect could be a reduction in local relative humidity causing membrane drying and an increase in HFR.

The information presented here can be used to optimize a fuel cell plate design. For automotive applications, the vehicle heat rejection capability is limited, so the fuel cell cannot be continuously operated at its peak power capability but is limited to about 0.55 V at the end of life or about 0.6 V at the beginning of life depending on the anticipated voltage degradation. As an example, the performance for the 0.5–1.0 land–channel flow field at 70 °C is shown in Fig. 9 where the power ($i \times V$), heat generation ($i \times (1.25 - V)$) and membrane to flow field temperature difference estimate are also included. For the membrane to flow field temperature difference estimate, a combined diffusion media bulk and contact resistance of 7.6 $cm^2\,K\,W^{-1}$ was used [9]. Although smaller land widths and narrower channel spans would be preferred, this flow field was selected as it probably best represents what can typically be achieved for automotive size stamped metal plates. The 70 °C condition was selected as this condition (relative humidity) had the highest performance. For vehicle applications, higher pressures are typically used to allow higher operating temperatures at similar relative humidities where the performance is maximized. This configuration achieved peak power at about 1.7 $A\,cm^{-2}$ or 0.5 V, but the design selection would need to be optimized for performance levels near 0.6 V to be within allowable vehicle heat rejection capabilities. Even at 0.6 V, configurations with narrower lands (and the same land fraction or resistance) had higher performance indicating that mass transfer is important under these conditions. As the cell voltage is driven below about 0.6 V, the heat generation rate exceeds the power generation rate and rapidly increases at higher current densities.

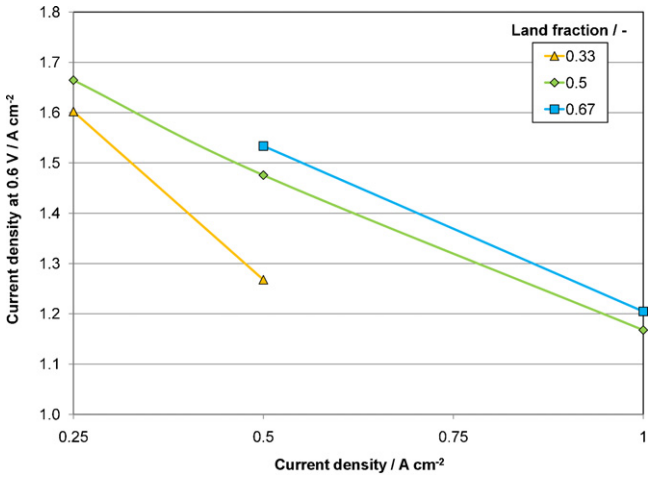

Fig. 10. Current density vs. land width and land fraction at 0.6 V and 70 °C.

The performance capabilities at 0.6 V at 70 °C as a function of land width for the tested land fractions are shown in Fig. 10. This figure more clearly illustrates the performance sensitivities to land width and land fraction. The performance increased consistently to the smallest land width tested (0.25 mm), so a performance plateau was not observed even though the diffusion distance through the DM thickness is becoming the longer than half the land width needed to diffuse to the MEA under the center of the land. Higher land fractions also had an improvement in performance due to the reduction in contact resistance. It should be noted that to achieve narrow lands while retaining higher land fractions requires that the channels also be narrow. Narrower channels would increase pressure drop. In this study, the channel depth was increased to compensate for this increase in flow resistance. However, in stamped plate flow fields, the channel depth is limited by metal forming limits. From a system perspective, the increase in performance from narrower lands and channels would need to be compared against the increase in parasitic compressor power to select the overall optimum configuration for the specific plate design and system operating conditions.

4. Conclusions

For performance at high current density, the land width was found to be the dominant factor. Reductions in land width to the smallest size tested (0.25 mm) continued to show improvement over wider lands. Adequate land fraction (preferably about 50%) was needed to provide low contact resistance. Therefore, the use of narrow lands to improve performance also requires narrow channels to provide an adequate land fraction. It was also found that channel spans should not be too large (more than about 1.0 mm), especially at lower land fractions, as this caused an undesirable increase in HFR. There was also an interaction between land fraction and operating conditions where flow fields with smaller land fractions performed better at limiting currents under wetter conditions, but had lower performance than larger land fraction flow fields at drier conditions. The results presented here can be used to evaluate the performance sensitivities to land widths and channel spans in order to optimize a fuel cell plate design.

References

[1] S.G. Goebel, Nested bipolar plate for fuel cell and method, US Patent 6974648 (2005).
[2] S.G. Goebel, J.A. Rock, Reactant feed for nested stamped plates for a compact fuel cell, US Patent 7291414 (2007).
[3] M. Oda, M. Mohri, H. Ohta, Y. Watanabe, S. Tanimoto, N. Saito, Fuel cell, US Patent Application 2008/0292941 (2008).
[4] F. Blank, T. Kunick, M. Schudy, Bipolar plate and fuel cell unit, US Patent Application 2009/0325036 (2009).
[5] Y.G. Yoon, W.Y. Lee, G.G. Park, T.H. Yang, Effects of channel and rib width of flow field plates on the performance of a PEMFC, Int. J. Hydrogen Energy 30 (2005) 1363–1366.
[6] J. Scholta, G. Escher, W. Zhang, L. Küppers, L. Jörissen, W. Lehnert, Investigation on the influence of channel geometries on PEMFC performance, J. Power Sources 155 (2006) 66–71.
[7] L. Wang, H. Liu, Separate measurements of current density under the channel and the shoulder in PEM fuel cells, J. Power Sources 180 (2008) 365–372.
[8] A. Higier, H. Liu, Optimization of PEM fuel cell flow field via local current density measurement, Int. J. Hydrogen Energy 35 (2010) 2144–2150.
[9] M. Khandelwal, M. Mench, Direct measurement of through-plane thermal conductivity and contact resistance in fuel cell materials, J. Power Sources 161 (2006) 1106–1115.